Supporting Information

Bromocriptine as a novel pharmacological chaperone for mucopolysaccharidosis IV A

Sergio Olarte-Avellaneda[1,2], Jacobo Cepeda Del Castillo[1], Andrés Felipe Rojas-Rodriguez[3], Oscar F. Sánchez[4], Alexander Rodríguez-López[1,5], Diego A. Suárez García[1,6], Luz Mary Salazar Pulido[6], Carlos J. Alméciga-Díaz[1,*]

[1] Institute for the Study of Inborn Errors of Metabolism, Faculty of Science, Pontificia Universidad Javeriana, Bogotá D.C., Colombia.

[2] Pharmacy Department, Faculty of Science, Universidad Nacional de Colombia, Bogotá D.C.

[3] Computational and Structural Biochemistry, Biochemistry and Nutrition Department, Faculty of Science, Pontificia Universidad Javeriana, Bogotá D.C., Colombia.

[4] Neurobiochemistry and Systems Physiology, Biochemistry and Nutrition Department, Faculty of Science, Pontificia Universidad Javeriana, Bogotá D.C., Colombia.

[5] Chemistry Department, Faculty of Science, Pontificia Universidad Javeriana, Bogotá D.C., Colombia.

[6] Faculty of Medicine, Universidad Nacional de Colombia, Bogotá D.C, Colombia.

[7] Chemistry Department, Faculty of Science, Universidad Nacional de Colombia, Bogotá D.C., Colombia.

Table of Contents

Experimental Procedures. including protein structure preparation, molecular docking, virtual screening, molecular dynamics, GALNS activity, inhibition assay, Recombinant GALNS in HEK293 cells, MPS IVA fibroblasts, Flow cytometry analysis, and Statistical analysis S2

Table S1. Top 20 hits of the compounds interacting with GALNS after virtual screening against the ZINC In Man subset from ZINC. S7

Figure S1. A. Geometrical isomers of Val283 in the GALNS protein structure. **B.** Molecular dynamics simulation for GALNS with both geometrical isomers of Val283. Insert figure shows the average of RMSD during the 100 ns simulation (t test, *** $p < 0.0001$, n=50001). S13

Figure S2. Protein-substrate interactions between human GALNS and keratan sulfate, chondroitin-6-sulfate, galactose-6-sulfate, and 4-methylumbelliferyl-β-d-galactopyranoside-6-sulfate (4MUGPS). Circle residues correspond to conserved interactions among all the substrates. Green and black residues are residues interacting through hydrogen bond and hydrophobic interactions, respectively. S14

References. S15

Experimental Procedures.

Protein structure. The crystallographic structure of human GALNS was obtained from the Protein Data Bank (PDB: 4FDI)[1] and modified using YASARA View v11.4.18[2] by removing water molecules, glycerol, and citric acid. Additional modifications, such as the formilglycine (FGly) at the position 79 and the calcium ion at the active site of the protein were manually added using subunit A. The protein was energetically minimized using Chimera version 1.12 with 100000 steepest descent steps, 0.001Å steepest descent step size, 10 conjugate gradient steps, 0.001 conjugate gradient step size and 10 updates per interval. The Gasteiger method and the AMBER ff14SB force field were used to assign and exchange standard residues. The method AM1-BCC was used to assign charges for all residues, the modified FGly (-1), and the calcium ion (+2). We also calculate the probability appearance of isomeric variants for the residue Val283 using the software MAESTRO academic version 11.8.012. Graphical comparison of the structures was done using Pymol version 2.0.7 for both angle changes and general structural comparison.

Molecular docking. State 1 geometrical probabilistic variant of Val283 for the GALNS structure was selected for molecular docking since a significantly lower root mean squared distance (RMSD) for the protein backbone was predicted after molecular dynamics simulation. Molecular docking was performed with galactose-6-sulfate (G6S), KS, C6S, and the artificial substrate 4-methylumbelliferyl-β-D-galactopyranoside-6-sulfate (4MUGPS) using Autodock vina[3]. The grid for the docking was centered between the calcium ion and the FGly embedded in the active cavity of the enzyme, with a size set to 20×20×20 for X, Y, and Z-axis, respectively. We evaluated the best 20 conformations for each of the ligands inside the GALNS active cavity and the results of ligand-protein interaction are reported as the affinity energy (kcal/mol). Interactions between substrates and GALNS crystal structure were predicted with LigPlot+ v.2.2[4].

Virtual screening. To identify potential PCs for GALNS, virtual screening was implemented using an in-house algorithm integrating Autodock vina, the ZINC In Man subset of ZINC [5] (11,421 compounds), and GALNS structure (state 1). Virtual screening was performed at the High-Performance Computing Center (ZINE) of Pontificia Universidad Javeriana. A structure-based clustering was performed for the Top 20 molecules by using the multidimensional scaling (MDS) algorithm available at ChemMine Web Tools[6]. Briefly, for MDS algorithm, atom pair descriptors (features) are generated for each compound, which are then used to calculate an all-against-all similarity matrix based on the common and unique features observed among all compound pairs using the Tanimoto coefficient (this coefficient has a range from 0 to 1 with higher values indicating greater similarity than lower ones). This similarity matrix is then converted into a distance matrix by subtracting each Tanimoto coefficient values from 1. Finally, coordinates are assigned to each molecule in a low-dimensional space to represent the distances graphically in a scatter plot[6].

Molecular dynamics. Molecular dynamics analysis was performed using GROMACS 4.5.5[7]. We analyzed the natural substrates, artificial ligand, and bromocriptine. GROMOS96 43a1 force field was used and the topology for the ligands was generated separately using Automated Topology Builder (ATB) and Repository version 2.2[8]. The simulation space was set as a cube filled with water solvent and a neutral net charge for the full system. The simulation time was set to 100 ns, and the trajectories were analyzed by RMSD (g_rms) and affinity energy (g_lie). All simulations were done at the High-Performance Computing Center (ZINE) of Pontificia Universidad Javeriana.

GALNS activity. GALNS activity was assayed by using the fluorogenic substrate 4MUGPS (Toronto Chemicals Research, North York, ON, Canada), and following a reported methodology[9]. One unit (U) was defined as the amount of enzyme catalyzing 1 nmol substrate per hour. Specific GALNS activity was expressed as U/mg of protein as determined by Lowry assay.

Inhibition assay. BC was kindly donated by BIOGEN® (Bogota, Colombia) and dissolved in DMSO for all the evaluations. The inhibitory effect of BC was assayed using a purified hrGALNS, which was produced in *P. pastoris* following our previously reported protocol [10, 11]. hrGALNS was co-incubated with the substrate 4MUGPS and various concentrations of BC during 18 h at 37 °C, followed by the detection of fluorescent product generation[9].

Recombinant GALNS in HEK293 cells. The effect of BC on the production of hrGALNS in mammalian cells was evaluated using HEK293 cells (ATCC CRL1573) transfected with the pCXN-GALNS plasmid. HEK293 cells were cultured in Dulbecco's modified medium (DMEM, Gibco, Thermo Fisher Scientific, Grand Island, NY, USA) supplemented with 15% fetal bovine serum (Eurobio, Les Ulis, France), penicillin 100 U/mL, and streptomycin 100 U/mL (Walkersville, MD, USA), at 37 °C in a 5% CO_2 incubator. Lipofectamine 2000 was used in the transfection following the manufacturer´s instructions (Invitrogen, Thermo Fisher Scientific, San Jose, CA, USA). BC was then added in a single pulse at different concentrations. Transfected cells treated with DMSO were used as control. GALNS activity was measured in cells lysate 48 h post-treatment.

MPS IVA fibroblasts. MPS IVA patient-derived skin fibroblasts (GM00593, GM00958, and GM01361) were obtained from the Coriell Institute (Camden, NJ). Cells were cultured as described above for the HEK293 cells. The effect of BC on GALNS activity in cells was done as previously reported[12]. The BC dilutions were added to the cells and incubated for 48 h followed by cell lysis using 1% sodium deoxycholate (Sigma-Aldrich, St. Louis, MO, USA). The enzyme activities of cell lysates were determined as described above. MPS IVA fibroblasts treated with DMSO were used as controls. All experiments were performed in triplicate.

Flow cytometry analysis. Cultured fibroblast cells, wild type, GM01361, and GM00593, were exposed to either 1 or 10 μM of BC for 36 h. Afterward, cells were labeled with Lysotracker™ Deep Red

(Molecular Probes, Thermo Fisher Scientific, San Jose, CA, USA) following the manufacturer's instructions. Cells were then analyzed on a FACSAria II (Becton Dickinson, CA, US). A 640 nm excitation laser line and a 660/20 nm Cy5 filter were used for capturing red fluorescent signals. All cytometry data were analyzed using FCS Express software (De Novo Software, Glendale, CA). Each experimental condition was analyzed in three independent biological replicates.

Statistical analysis. The results are shown as the mean ± the standard deviation (S.D.) and were analyzed by t-test or ANOVA followed by the Holm-Šidák test when appropriate. Differences between groups were considered significant when $p < 0.05$ on GraphPad PRISM 7.0.

Table S1. Top 20 hits of compounds interacting with GALNS after virtual screening against the ZINC In Man subset from ZINC.

Rank	ZINC ID	Name / Structure	Molecular Weight (g/mol)	Affinity energy (kcal/mol)	Target/Activities (based on ChEMBL 20)	Side effects (Top five side effects reported in SIDER[13] and/or VigiAccess[14] databases)
1	ZINC53683151	Bromocriptine 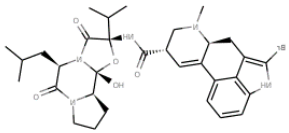	654.6	-10.8	• D(2) dopamine receptor • 5-hydroxytryptamine receptor 1A • D(3) dopamine receptor • 5-hydroxytryptamine receptor 6 • Alpha-1D adrenergic receptor	• Dizziness (7-49%) • Lightheadedness (5%) • Abdominal cramps (4%) • Anorexia (4%) • Vomiting (2-5%)
2	ZINC02015955	Tarazepide 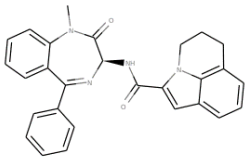	448.5	-10.6	• CCK-A receptor • Histamine H2 receptor	• No reported or unknown.
3	ZINC71928211	Bromocriptine 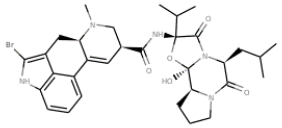	654.6	-10.5	• D(2) dopamine receptor • 5-hydroxytryptamine receptor 1A • D(3) dopamine receptor • 5-hydroxytryptamine receptor 6 • Alpha-1D adrenergic receptor	• The same as Rank #1

Rank	ZINC ID	Name / Structure	Molecular Weight (g/mol)	Affinity energy (kcal/mol)	Target/Activities (based on ChEMBL 20)	Side effects (Top five side effects reported in SIDER[13] and/or VigiAccess[14] databases)
4	ZINC00601275	Talniflumate 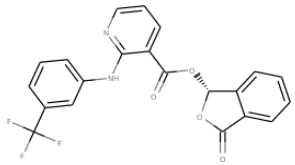	414.3	-10.4	• Non-steroidal anti-inflammatory analgesic • Anti-inflammatory • Relaxin receptor 1 • Relaxin receptor 2	• Dyspepsia (11%) • Somnolence (11%) • Dizziness (11%) • Nausea (10%) • Pruritus (9%) • Myocardial infarction[15] • Chronic kidney disease[16]
5	ZINC04212887	Dexamethasone-21-sulfobenzoate 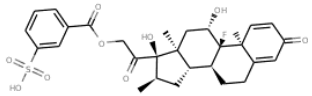	576.6	-10.4	• Progesterone receptor • Mineralocorticoid receptor • Glucocorticoid receptor	• Pneumonia (5%) • Nausea (4%) • Diarrhoea (4%) • Pyrexia (3%) • Fatigue (3%)
6	ZINC03872491	(8S,9S,13R,14S,16S,17R)-13-Methyl-6,7,8,9,11,12,14,15,16,17-decahydrocyclopenta[a]phenanthrene-3,16,17-triol 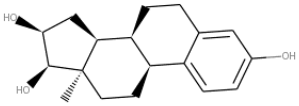	288.3	-10.3	• Sulfotransferase • Sex hormone-binding globulin • Estrogen receptor • Corticosteroid-binding globulin	• No reported or unknown.
7	ZINC01847292	Devazepide 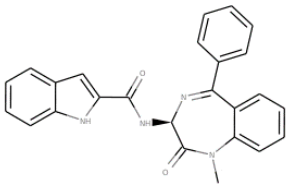	408.4	-10.2	• Cholecystokinin receptor type A • Gastrin/cholecystokinin type B receptor • Neurogenic locus notch homolog protein 1, 2, 3 and 4 • Calcitonin gene-related peptide type 1 receptor	• No reported or unknown.

Rank	ZINC ID	Name / Structure	Molecular Weight (g/mol)	Affinity energy (kcal/mol)	Target/Activities (based on ChEMBL 20)	Side effects (Top five side effects reported in SIDER[13] and/or VigiAccess[14] databases)
8	ZINC14880002	Dihydroergotoxine 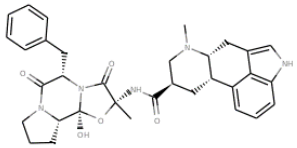	583.6	-10.1	• 5-hydroxytryptamine receptor 5A • Somatostatin receptor type 2 • Somatostatin receptor type 1	• Nausea (15%) • Dizziness (9%) • Headache (8%) • Vomiting (8%) • Rash (8%)
9	ZINC04172334	Algestone Acetophenide 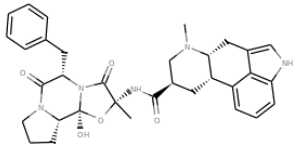	448.6	-10.1	• Nuclear receptor subfamily 1 group I member 3 • Solute carrier organic anion transporter family member 1A1 • Fatty acid-binding protein, liver • Mineralocorticoid receptor	• Headache (14%) • Metrorrhagia (13%) • Dizziness (8%) • Menstrual disorder (8%) • Abdominal pain (6%)
10	ZINC00538404	(6S,12ar)-Tadalafil 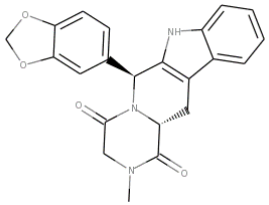	389.4	-10.1	• Phosphodiesterase 5 inhibitor • Dual 3',5'-cyclic-AMP and -GMP phosphodiesterase 11A • cGMP-specific 3',5'-cyclic phosphodiesterase	• Headache (3-42%) • Nausea (10-11%) • Respiratory tract infection (5-13%) • Sinus congestion (9%) • Pulmonary hypertension(8%)
11	ZINC26167988	Nimorazole 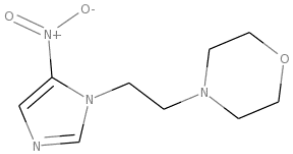	226.2	-10.0	• Antibacterial • Radiosensitizing activity • Replicative DNA helicase	• Nausea (12%) • Vomiting (10%) • Diarrhea (9%) • Dizziness (7%) • Paresthesia (7%)

Rank	ZINC ID	Name / Structure	Molecular Weight (g/mol)	Affinity energy (kcal/mol)	Target/Activities (based on ChEMBL 20)	Side effects (Top five side effects reported in SIDER[13] and/or VigiAccess[14] databases)
12	ZINC27305632	Plevitrexed 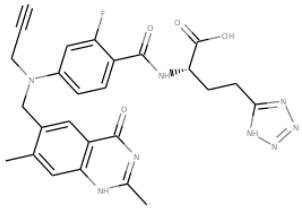	532.5	-10.0	• Thymidylate synthase • Dihydrofolate reductase • Antineoplastic	• Thrombocytopenia (20%) • Neutropenia (10%) • Pancytopenia (10%) • Pyrexia (10%) • Scleroderma (10%)
13	ZINC03995861	Picrotin 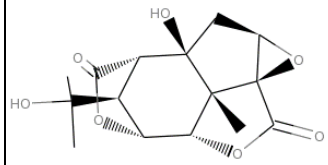	310.3	-10.0	• Glycine receptor subunit alpha-1, 2 and 3. • Pore blocker	• No reported or unknown.
14	ZINC64033452	Lumacaftor 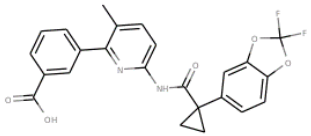	452.4	-9.9	• Cystic fibrosis transmembrane conductance regulator • Class I corrector	• Dyspnea (43%) • Diarrhea (22%) • Nausea (17%) • Bronchospasm (17%) • Abdominal pain (13%)
15	ZINC11677911	Bisoctrizole 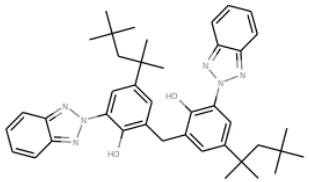	658.8	-9.9	• UV filter	• No reported or unknown.

Rank	ZINC ID	Name / Structure	Molecular Weight (g/mol)	Affinity energy (kcal/mol)	Target/Activities (based on ChEMBL 20)	Side effects (Top five side effects reported in SIDER[13] and/or VigiAccess[14] databases)
16	ZINC34375693	Palosuran 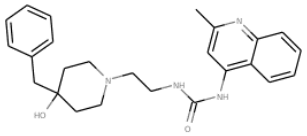	418.5	-9.9	• Urotensin-2 receptor antagonist • D(3) dopamine receptor	• Headache (20%) • Nausea (10%) • Vomiting (10%) • Dizziness (10%) • Sweating (10%)
17	ZINC03978005	Dihydroergotamine 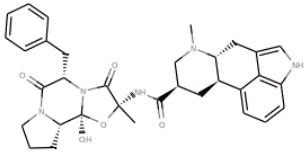	583.6	-9.9	• 5-hydroxytryptamine receptor 1A • Alpha-2A adrenergic receptor • D(2) dopamine receptor • D(1A) dopamine receptor • Acute migraine therapy	• Nausea (7%) • Vomiting (5%) • Chest pain (4%) • Pain (3%) • Abdominal pain (3%)
18	ZINC71928212	Bromocriptine 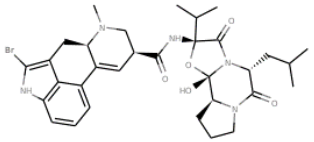	654.6	-9.9	• D(2) dopamine receptor • 5-hydroxytryptamine receptor 1A • D(3) dopamine receptor • 5-hydroxytryptamine receptor 6 • Alpha-1D adrenergic receptor	• The same as Rank #1
19	ZINC53282743	Ergocristine 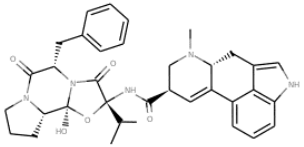	609.7	-9.8	• Alpha-2A adrenergic receptor • 5-hydroxytryptamine receptor 1E and 2B	• N.A.* * Illegal drug. It is a Schedule I drug of the Controlled Substances Act.

Rank	ZINC ID	Name / Structure	Molecular Weight (g/mol)	Affinity energy (kcal/mol)	Target/Activities (based on ChEMBL 20)	Side effects (Top five side effects reported in SIDER[13] and/or VigiAccess[14] databases)
20	ZINC04217252	Penfluridol 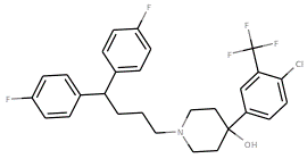	523.9	-9.8	• D(3) dopamine receptor • D(1B) dopamine receptor • Nociceptin receptor • Antipsychotic	• Extrapyramidal disorders (11%) • Somnolence (5%) • Tremor (4%) • Akathisia (4%) • Dyskinesia (4%)

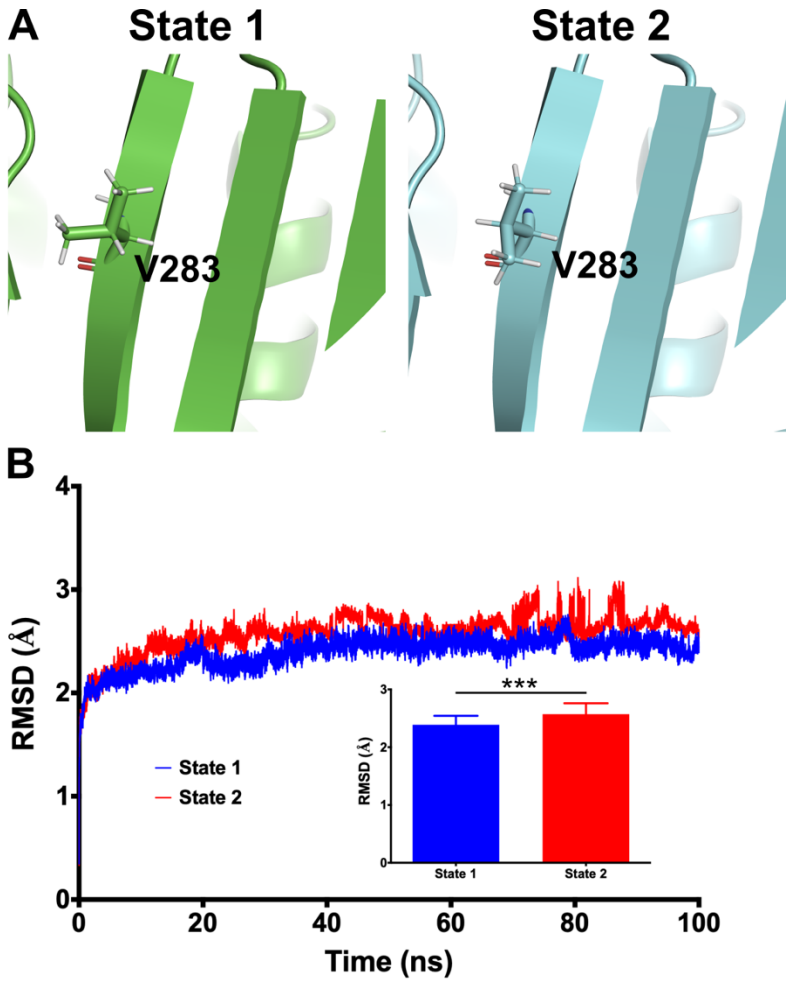

Figure S1. A. Geometrical isomers of Val283 in the GALNS protein structure. **B.** Molecular dynamics simulation for GALNS with both geometrical isomers of Val283. Insert figure shows the average of RMSD during the 100 ns simulation (t test, *** $p < 0.0001$, n=50001).

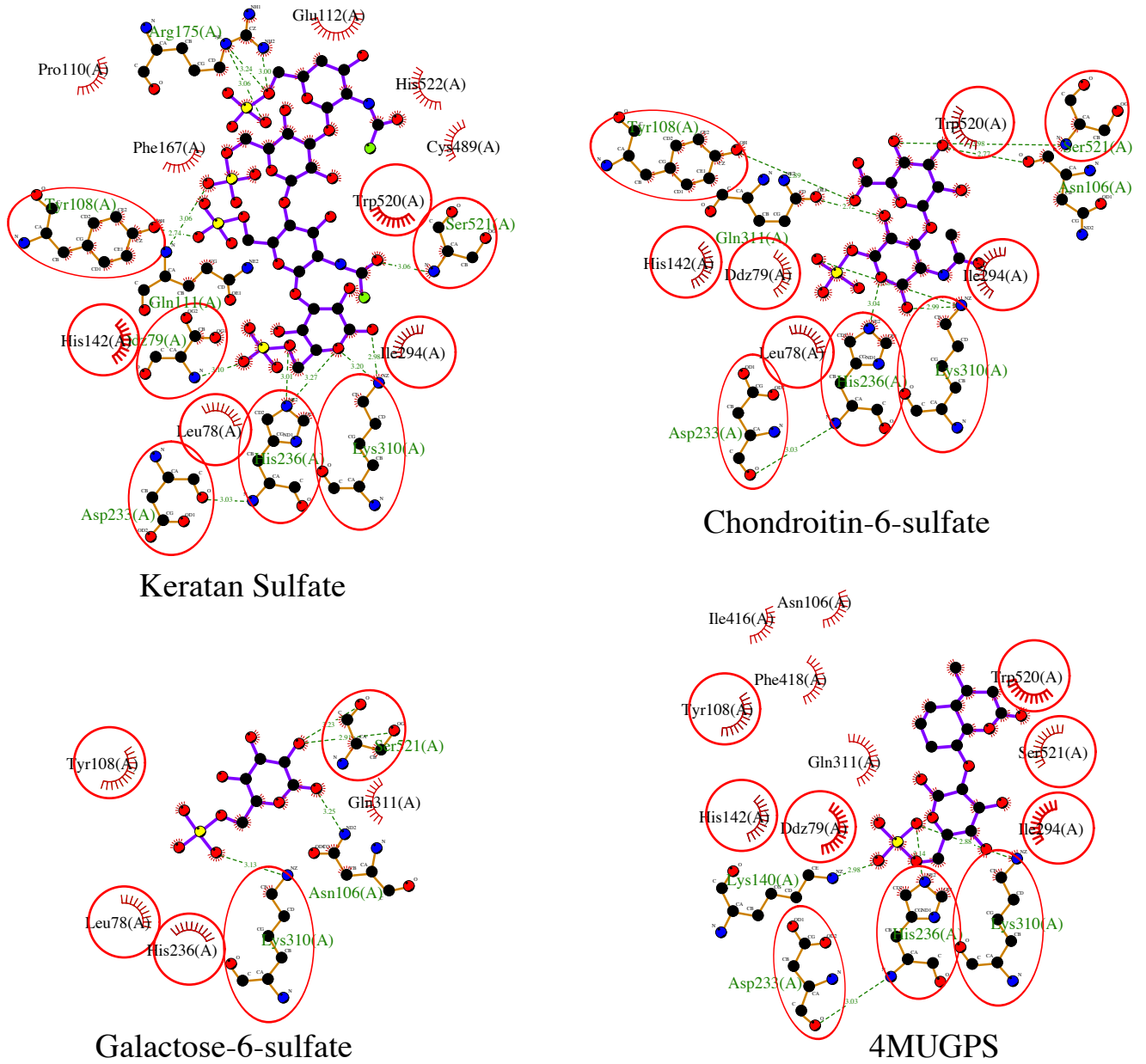

Figure S2. Protein-substrate interactions between human GALNS and keratan sulfate, chondroitin-6-sulfate, galactose-6-sulfate, and 4-methylumbelliferyl-β-d-galactopyranoside-6-sulfate (4MUGPS). Circle residues correspond to conserved interactions among all the substrates. Green and black residues are residues interacting through hydrogen bond and hydrophobic interactions, respectively.

References

[1]. Rivera-Colon, Y.; Schutsky, E. K.; Kita, A. Z.; Garman, S. C., The structure of human GALNS reveals the molecular basis for mucopolysaccharidosis IV A. *J. Mol. Biol.* **2012,** *423* (5), 736-751.

[2]. Krieger, E.; Vriend, G., YASARA View - molecular graphics for all devices - from smartphones to workstations. *Bioinformatics* **2014,** *30* (20), 2981-2982.

[3]. Trott, O.; Olson, A. J., AutoDock Vina: improving the speed and accuracy of docking with a new scoring function, efficient optimization, and multithreading. *J. Comput. Chem.* **2010,** *31* (2), 455-461.

[4]. Laskowski, R. A.; Swindells, M. B., LigPlot+: multiple ligand-protein interaction diagrams for drug discovery. *J. Chem. Inf. Model.* **2011,** *51* (10), 2778-2786.

[5]. Irwin, J.; Sterling, T.; Mysinger, M.; Bolstad, E.; Coleman, R., ZINC: a free tool to discover chemistry for biology. *J. Chem. Inf. Model.* **2012,** *52* (7), 1757-1768.

[6]. Backman, T. W.; Cao, Y.; Girke, T., ChemMine tools: an online service for analyzing and clustering small molecules. *Nucleic Acids Res.* **2011,** *39* (Web Server issue), W486-491.

[7]. Pronk, S.; Pall, S.; Schulz, R.; Larsson, P.; Bjelkmar, P.; Apostolov, R.; Shirts, M. R.; Smith, J. C.; Kasson, P. M.; van der Spoel, D.; Hess, B.; Lindahl, E., GROMACS 4.5: a high-throughput and highly parallel open source molecular simulation toolkit. *Bioinformatics* **2013,** *29* (7), 845-854.

[8]. Malde, A. K.; Zuo, L.; Breeze, M.; Stroet, M.; Poger, D.; Nair, P. C.; Oostenbrink, C.; Mark, A. E., An automated force field topology builder (ATB) and repository: version 1.0. *J. Chem. Theory. Comput.* **2011,** *7* (12), 4026-4037.

[9]. van Diggelen, O. P.; Zhao, H.; Kleijer, W. J.; Janse, H. C.; Poorthuis, B. J.; van Pelt, J.; Kamerling, J. P.; Galjaard, H., A fluorimetric enzyme assay for the diagnosis of Morquio disease type A (MPS IV A). *Clin. Chim. Acta* **1990,** *187* (2), 131-139.

[10]. Rodríguez-López, A.; Alméciga-Díaz, C. J.; Sánchez, J.; Moreno, J.; Beltran, L.; Díaz, D.; Pardo, A.; Ramírez, A. M.; Espejo-Mojica, A. J.; Pimentel, L.; Barrera, L. A., Recombinant human N-acetylgalactosamine-6-sulfate sulfatase (GALNS) produced in the methylotrophic yeast Pichia pastoris. *Sci. Rep.* **2016,** *6*, 29329-29342.

[11]. Rodriguez-Lopez, A.; Pimentel-Vera, L. N.; Espejo-Mojica, A. J.; Van, H. A.; Tiels, P.; Tomatsu, S.; Callewaert, N.; Almeciga-Diaz, C. J., Characterization of human recombinant N-acetylgalactosamine-6-sulfate sulfatase produced in Pichia pastoris as potential enzyme for mucopolysaccharidosis IVA treatment. *J. Pharm. Sci.* **2019,** *108* (8), 2534-2541.

[12]. Almeciga-Diaz, C. J.; Hidalgo, O. A.; Olarte-Avellaneda, S.; Rodriguez-Lopez, A.; Guzman, E.; Garzon, R.; Pimentel-Vera, L. N.; Puentes-Tellez, M. A.; Rojas-Rodriguez, A. F.; Gorshkov, K.; Li, R.; Zheng, W., Identification of ezetimibe and pranlukast as pharmacological chaperones for the treatment of the rare disease mucopolysaccharidosis type IVA. *J. Med. Chem.* **2019,** *62* (13), 6175-6189.

[13]. Kuhn, M.; Letunic, I.; Jensen, L. J.; Bork, P., The SIDER database of drugs and side effects. *Nucleic Acids Res.* **2016,** *44* (D1), D1075-D1079.

[14]. WHO Collaboration Centre for International Drug Monitoring. VigiAccess. http://www.vigiaccess.org/ (accessed May 2020).

[15]. Salvo, F.; Antoniazzi, S.; Duong, M.; Molimard, M.; Bazin, F.; Fourrier-Réglat, A.; Pariente, A.; Moore, N., Cardiovascular events associated with the long-term use of NSAIDs: a review of randomized controlled trials and observational studies. *Expert Opin. Drug Saf.* **2014,** *13* (5), 573-585.

[16]. Winkelmayer, W. C.; Waikar, S. S.; Mogun, H.; Solomon, D. H., Nonselective and cyclooxygenase-2-selective NSAIDs and acute kidney injury. *Am. J. Med. Stud.* **2008,** *121* (12), 1092-1098.